



Research Article


A geo-spatial assessment of drought impacts on forest cover in yabello forest, in the semi-arid region of Ethiopia



Bayisa Negasa Wolteji¹  · Fayera Gizawu Garbaba¹

Received: 29 December 2022 / Accepted: 12 April 2023

Published online: 26 April 2023

© The Author(s) 2023 

Abstract

Drought is a key challenge for third-world countries whose economies are based on agriculture. Also, lack of rainfall plays a major role in accelerating climate change. Drought is resulting in a decline in vegetation greenness and plant mortality specifically in the semi-arid region. In this study, satellite-based drought assessment was used to characterize drought and its impact on forests in the semi-arid regions of Ethiopia. Drought severity and forest cover change were detected over the period between 2014 and 2022 Using geographic information systems and remote sensing techniques. Vegetation condition index (VCI) and Normalized difference vegetation index (NDVI) were used to detect drought severity in the present study. Results of this study showed that 2017, 2015, 2022 and 2019 were the most drought years. The forest resource is significantly decreased during severe drought years. The Minimum dense forest was observed in 2017 and 2015 over a spatial extent of 193 ha and 217 ha respectively during drought years. To evaluate how precipitation deficit affects forest function, simple linear regression is performed. Results of this linear regression " $R^2 = 0.49$ and $P = 0.05$ " indicated that nearly 50% of forest greenness is influenced by precipitation deficit. This study suggested that remote sensing indices are very crucial to characterize drought patterns at a small "scale", particularly in the assessment of drought impact on forest resources.

Article Highlights

- Satellite indices like NDVI and VCI help to monitor the drought impact on forest cover.
- When severe drought is occurred along with precipitation deficit, the forest cover is decreased.
- Remote sensing data provide clear information for decision-making regarding drought's impact on the forest.

Keywords NDVI · Precipitation · Relationship · VCI · Vegetation

1 Introduction

Drought is described as a situation when there is insufficient precipitation or lack of enough water which affects vegetation greenness and health, plant mortality, reduced

water levels, and other adverse ecological and/or biophysical conditions [1, 2]. Water-stressed plants typically close stomata to reduce water loss and prevent the development of excessively low water potentials, which significantly affect photosynthesis activity. This situation result in

✉ Bayisa Negasa Wolteji, bayisajs2017@gmail.com; Fayera Gizawu Garbaba, gfayegis@gmail.com | ¹Department of Earth Science, Wollega University, P.O. BOX 395, Nekemte City, Ethiopia.



carbon stress, reduced growth, and greater susceptibility to insects, disease, and plant mortality [3, 4]. Rapidly the decrement in forest areas is negatively affected ecosystem function because there is a strong relationship between forest and ecosystem components. Changing environmental conditions and nutrients can affect the biota and related services provided by forests. Species disturbances, migration and extinction can happen as a result of forest degradation along with climate changes [5-7]. Therefore, gathering information required to monitor this natural resource is of utmost importance to maintain biodiversity conservation [8].

In recent decades, remotely sensed normalized difference vegetation index (NDVI) is used as a proxy for earth vegetation productivity that allows for continuous and long-term monitoring of information on the relationship between vegetation and climate and is one of the most widely used indicators in studies involving vegetation dynamics and ecosystem health across the world [9, 10]. Monitoring and assessing droughts in the semi-arid region at high resolution is also required the use of Remote Sensing based data and methods to fill a gap in in-situ data due to the drawbacks of using only ground-based data, such as inadequate spatial and temporal coverage of meteorological station data [11].

Changes in vegetation cover have attracted a focus of researchers to the assessment of vegetation response to changes in air temperature, precipitation, solar radiation, and sea surface temperature [12].

Precipitation variability is extra-ordinarily responsible for vegetation change in vegetation-atmosphere interactions when compared to the aforementioned climate variable due to the great role that precipitation plays in water availability. It is the leading factor controlling ecosystem structure and driving biological processes on over 40% of the earth's vegetated surfaces [13, 14].

Moreover, examining the relationship between NDVI and climate variables helps us to recognize the most influential climatic variable in a particular region [15].

In Ethiopia, many studies have highlighted differences in NDVI changes and their response to climatic factors [16-18]. Therefore, those studies suggested that rainfall is the most crucial element to characterize the impact of drought on the environment in east Africa, particularly the semi-arid region of Ethiopia. In Ethiopia even though the relationship between remote sensing indices and precipitation was evaluated, the relationship between them has been not recognized at a small scale with improved resolution. In another way, many studies assessed agricultural drought using remote sensing indices from medium to large scale [15, 19, 20]. All previous studies reported

that crop yield has declined as a result of drought severity specifically in the lowland region of Ethiopia. Although the importance of satellite indices is well recognized to assess drought impact on agriculture from medium scale to large scale, assessment of drought impact on forest resource at small scale has not been recognized.

Furthermore, several studies found that forests have been depleted as a result of anthropogenic activity in many regions of the country without considering drought impact on the forest ecosystem, using remote sensing Spatio-temporal forest change detection techniques [21-24]. Therefore, the novelty of this study is the time series analysis of drought severity assessment and its impact on the Yabello forest, using satellite drought indices, and assessing the relationship between forest and precipitation.

2 Materials and methods

2.1 Study area description

This study was conducted on the drought-prone region of Ethiopia, the Yabello forest, and its surrounding. The forest is located in the Yabello district of Borana Zone, southern Oromia. The total area of the study sites is 26,956.7 ha and its altitude range between 1438 and 2354 m. m.s.l [25]. The absolute location of this area lies between 4° 45' 0" N to 4° 57' 0" N and 38° 1' 0" E to 38° 10' 30" E (Fig. 1). The Yabello district has a bi-modal rainfall pattern with the main rainy season between March and May with high precipitation in April. The mean annual rainfall of the district is 587.2 mm. The mean annual temperature varies from 15 to 24 °C and shows little variation across the seasons [26]. At the Zonal level, the mean annual precipitation of the zone ranges from 352 mm in the southern part to 605 mm to the northern part of the zone. Geologically, most of the area which accounts for 40% is dominated by quaternary deposits, 38% basement complex formations, and 20% volcanic [27]. The region has a semi-arid savannah landscape, marked by gently sloping lowlands and flood plains vegetated predominantly with grass and bush-land. According to [27], this study area comprises three main soil types, 53% loam soil, 30% black clay, volcanic light-colored silty clay, and 17% silty. Five major land use/covers, namely; grassland, woody vegetation, cultivated, settlement, and bare land were identified in the district [22, 28]. Evergreen and semi-evergreen bush-land and thickets, rangeland dominated by shrubby *Acacia*, *Commiphora*, and allied genera, and dwarf shrub grassland to shrub grassland are also found in the area. The district has a total population of about 128,762 (64,692 Males and 64,070 Females) [29].

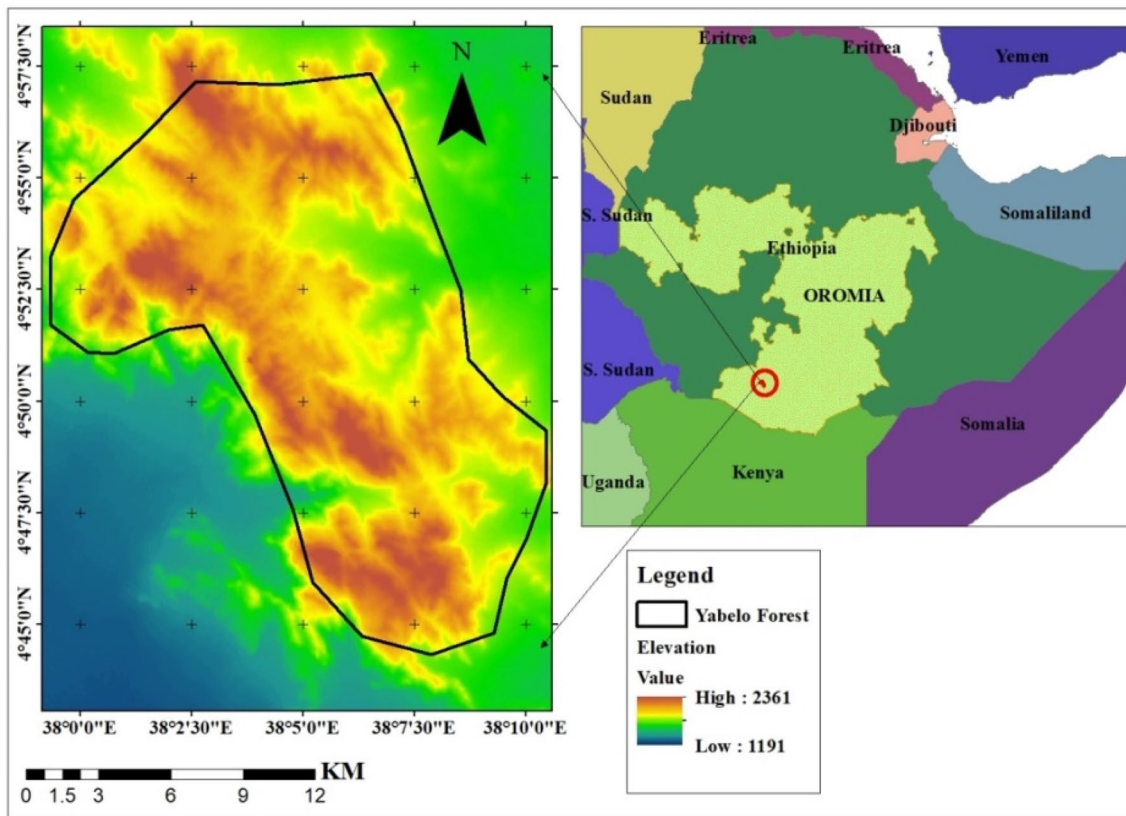


Fig. 1 Map of Yabelo forest

Table 1 Specifications of Landsat data used in the study

	Path raw	September	October	November	Resolution	Year	Source
Landsat 8	168_57	18	19	07	30 m	2014	https://www.usgs.gov
Landsat 8	168_57	05	06	10	30 m	2015	https://www.usgs.gov
Landsat 8	168_57	08	–	28	30 m	2016	https://www.usgs.gov
Landsat 8	168_57	10	11	31	30 m	2017	https://www.usgs.gov
Landsat 8	168_57	13	15	31	30 m	2018	https://www.usgs.gov
Landsat 8	168_57	16	01	21	30 m	2019	https://www.usgs.gov
Landsat 8	168_57	19	20	–	30 m	2020	https://www.usgs.gov
Landsat 8	168_57	05	06	26	30 m	2021	https://www.usgs.gov
Landsat 8	168_57	24	09	05	30 m	2022	https://www.usgs.gov

2.2 Data sources

In the present study, Landsat 8 OLI/TIRS with a 30-m spatial resolution (www.usgs.gov) was used as the data source to calculate NDVI and used to generate LULC, from the year 2014 to 2022. Since satellite images are application specific Landsat 8 is capable to detect forest cover changes at a small scale. These years were selected based on forest area a demarcated year and data availability. A total of twenty-two Landsat data was downloaded during the short rainy season (September to November) and for

each month cloud-free satellites were downloaded in 2016 and 2020 more than 10% of cloud free data were omitted, and the mean of NDVI was used for each year (Table 1). This season was selected because of its higher rainfall variability [26]. Additionally, the most common statistical methods applied to time series of NDVI and precipitation, such as simple linear correlation or regression analyses; produce inaccurate results if seasonality is not taken into account [30]. Therefore, this research was undertaken to demonstrate a statistical modeling technique that would

account for the seasonal timing effects of precipitation on the forest.

The CHIRPS rainfall data was downloaded from the Famine Early Warning Network (FEWS). CHIRPS is a quasi-global (50°S–50°N) gridded product available from 1981 to near present at 0.05° spatial resolution (~5.3 km) and at daily, pentadal, decadal, and monthly temporal resolution. It is developed by the U.S. Geological Survey (USGS) and the Climate Hazards Group (CHG) at the University of California [31]. Data were downloaded from 2014 to 2022 during the short rainy season (September to November) from the CHG web page (<http://chg.geog.ucsb.edu/data/chirps/index.html>). [32] used CHIRPS rainfall data for validating the drought monitoring tool in food-insecure regions of Ethiopia. In the same way, CHIRPS rainfall data was validated and showed the best performance than other rainfall data sources in Ethiopia [33, 34]. In this study, CHIRPS rainfall data was used for linear regression analysis between NDVI and precipitation.

2.3 Data analysis

2.3.1 NDVI calculation

During the early 1980s, the NDVI was defined and developed by scientists at NASA's Goddard Space Flight Center, Greenbelt, Md. for monitoring vegetation health based on the difference between absorption and reflectance of green leaves of the red and near-infrared band of visible light, respectively[35]. The value of NDVI of each pixel is estimated by dividing the reflectance difference by the sum between NIR and the Red band. Its value range between - 1 and + 1, and lower values/near to zero represent stressed vegetation, negative values represent open water or high moisture content, and + 1 indicates healthy vegetation cover, respectively. Seasonal NDVI (September to November) was used in this study. To calculate NDVI indices from Landsat data, there are the pre-requested procedure which is guided by USGS, these include;

VNIR spectral radiance data were converted to top of atmosphere planetary reflectance using the reflectance rescaling coefficient provided in the Landsat Metadata file. The following equation is used to convert DN values to the top of atmosphere reflectance for the Landsat image.

$$\rho\lambda = M\rho \times Q_{cal} + A\rho \tag{1}$$

where $\rho\lambda$ =TOA planetary reflectance without correction for the solar angle.

Table 2 VCI and Drought severity class

VCI range (%)	Drought severity class
> 40	No drought
30–40	Mild drought
20–30	Moderate drought
10–20	Severe drought
0–10	Extreme drought

$M\rho$ = represents a band-specific multiplicative rescaling factor from the Metadata Reflectance Multi-Band X where X is the band number.

Q_{cal} is quantized and calibrated standard product pixel value (DN).

$A\rho$ represents the band-specific additive rescaling factor from Metadata Reflectance-Add-Band-X, where X is the band number. The next procedure is correcting the reflectance value with the sun angle.

The formula for correcting this value is;

$$\rho\lambda = \frac{\rho\lambda}{\cos\theta_{SZ}} = \frac{\rho\lambda}{\sin\theta_{SE}} \tag{2}$$

where $\rho\lambda$ = TOA-planetary reflectance. θ_{SE} = local sun elevation angle, the scene center sun elevation angle in degrees is provided in metadata (sun elevation).

The local zenith angle is calculated as Eq. (3)

$$90^\circ - \theta_{SE} \tag{3}$$

To obtain more accurate results, its unit should be converted from radian to degree. These procedures were carried out for all bands used in this study which operate in the optical region of the electromagnetic spectrum (bands 4 and 5). Finally, after these corrections were completed bands were extracted into the study area by using an ArcGIS extraction tool. Then NDVI was generated by using an ArcGIS raster calculator.

$$NDVI = \frac{NIR - RED}{NIR + RED} \tag{4}$$

2.3.2 Vegetation condition index

VCI is useful for vegetation condition assessment, as it assesses changes in NDVI through time since vegetation is water-stressed due to water deficiency such as during drought as stated by [36].

According to Kogan-VCI is measured as a percentage with values ranging between 0 (Lowest) and 100 (Highest) as in Eq. 5 with values equal to or below 40% considered as drought to varying degrees of severity (Table 2).

Therefore, in the present study drought severity during the growing season (short rainy season) was measured using the NDVI-based Vegetation Condition Index (VCI) for 8 years, for the same period using the ArcGIS raster calculator tool as in Eq. (5).

$$VCI = 100 \times \frac{NDVI - NDVI_{min}}{NDVI_{max} - NDVI_{min}} \quad (5)$$

where

NDVI = the value of NDVI at the time of observation.

NDVI min = Absolute minimum NDVI value of 8 years.

NDVI max = Absolute maximum NDVI value of 8 years.

2.3.3 Forest cover change

To access drought's impact on the forest, forest cover change was evaluated during the study period. Land use/land cover of 2021 was used as the reference to evaluate the variability of forest cover change as the result of drought. This year was selected because a large portion of the region was covered by forest and to minimize the contribution of settlement and agricultural activity in the result of this finding.

Recently, settlement and agricultural activity are rapidly increasing. Therefore, in this study settlement and others human activities were maxed out from the study area to identify drought impact on the forest region by omitting the impact of anthropogenic activities. Land use/land covers were classified based on the NDVI classification range as used by [37] at twelve districts of Ethiopia, which belong to the same drought-prone area. These NDVI ranges were $> = -0.3 < = 0.084$ is a water body, $> 0.084 < 0.18$ is bare land, $> = 0.18 < 0.3$ is sparse vegetation, and $> = 0.3 < 0.6$ is dense vegetation. Based on these NDVI ranges spatial-temporal forest covers were evaluated over 8 time series years using ArcGIS image analysis.

2.3.4 Correlation analysis between precipitation and NDVI

A simple linear regression model was applied to examine how the precipitation–NDVI, relate to each other based on their mean values using “Microsoft excel”. The mean values for both variables for each year were evaluated.

Besides, the Pearson correlation matrix was applied to evaluate the relationships of an index. The linear regression model was computed as follows.

$$Y_i = \beta_0 + \beta_1 X_i + \varepsilon_i \quad (6)$$

where

$Y_i = NDVI$, for the i th period, $X_i =$ precipitation, $\beta_0 + \beta_1 X_i =$ linear relationships between Y_i and X_i , $\beta_0 =$ mean of Y_i when $X = 0$ (intercept), $\beta_1 =$ change in the mean of Y when X increases by 1 (slope), $\varepsilon_i =$ random error term.

The results of simple linear regression or Pearson correlation can be positive or negative. This ranges between 0 and + 1. Regression or Pearson correlation values close to zero indicate no relationship between the indices. However, if one index increases as the other index (e.g., NDVI) decreases, then the relationship is negative (Fig. 2).

3 Results

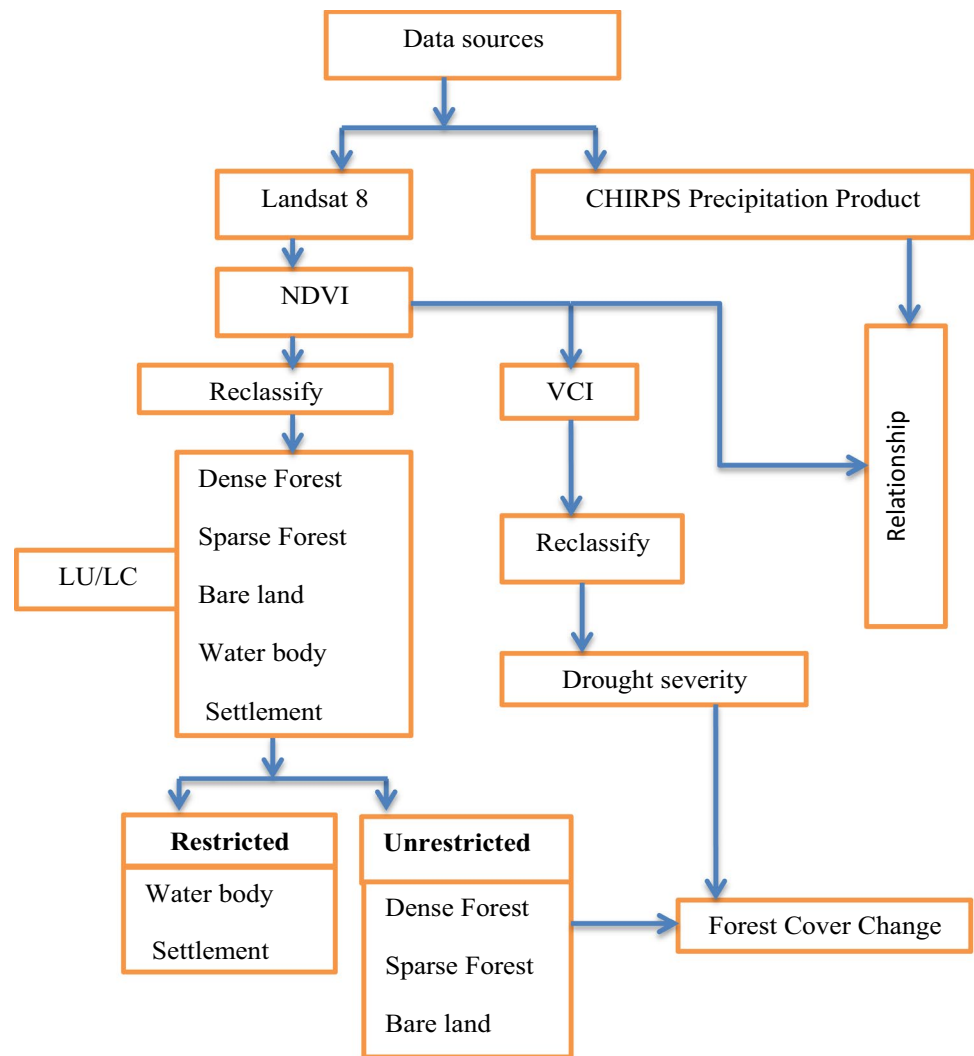
3.1 Drought severity

The vegetation condition index revealed drought years over the study area during the study period.

Accordingly, the most drought years were detected in 2015, 2017, 2019, and 2022 years as it's shown in Fig. 3. Spatially, in 2015, 2017, 2019, and 2022 years, severe drought covered 177.5 ha, 537.9 ha, 69.7 ha, and 80.6 ha corresponding to the aforementioned years (Table 3). Northwest, central, and southeast of the forest were frequently affected as the result of drought (Fig. 3). Also moderate drought was detected in these years over the spatial magnitude of 2,994.49 ha, 7,116.2 ha, 7,359.7 ha, and 4,449.6 ha corresponding to above years. In these years, only 1,397 ha, 4420.7 ha, 8,563.7 ha, and 14,381.4 ha were not affected by drought (Table 3).

The wettest years were also identified during the study period. For example, in 2014 even though a severe drought occurred over 80.1 ha, a large portion of the region (15,783.7 ha) remained normal (Table 3). In 2016, severe drought covered only 7.6 ha, and moderate drought covered 665.3 ha whereas, a larger area (19,048.7 ha) remained without being affected by drought. In 2018, severe drought covered 43.6 ha, moderate drought covered 1,591.2 ha of the Yabalo forest, and 15,581.2 ha was not affected by drought (Table 3). Similarly, in 2020 and 2021, severe drought did not occur in the Yabalo forest. In 2020, only 37.9 ha belonged to moderate drought stress, and the maximum spatial extent of the wettest forest condition (24,644.2 ha) was detected this year. In 2020, 37.9 ha moderate drought might be indicated that forests are recovering from the drought that occurred in 2019 (Table 3). Even though severe drought was not recorded in 2021, there was an implication to drought occurrence from analyzed data. For instance, the maximum normal forest coverage in 2020 (24,644.2 ha) was decreased to 18,403.5 ha in 2021. Also, the mild drought of 269.9 ha in 2020 increased to 6,568.5 ha

Fig. 2 Methodological flow-chart of the study



in 2021. In 2021, moderate, mild, and normal drought categories covered 4.3 ha, 6,568.5 ha, and 18,403.5 ha of land respectively (Table 3). Following 2021, drought severity was detected in the region in 2022. In 2022 severe, moderate, mild, and normal forest land mass expanded over 80.6 ha, 4,449.6 ha, 6,050.3 ha, and 14,381.4 ha respectively. In all of the detected drought year, the northwest, central, and southeast of the forest was the most affected portions of the Yabelo forest (Fig. 3).

3.2 Impact of drought on forest

NDVI-based LU/LC revealed that forest cover has been not stable during the study period. For instance, as indicated in Table 4 in 2014 dense forest, sparse forest, and bare land covered 305 ha, 19,660 ha, and 4,995 ha respectively. But following 2014, in 2015 the dense forest was decreased while sparse forest and bare land were increased. This is maybe because of the drought that occurred in the

Yabello forest in 2015. The dense forest was decreased by 88 ha and bare land was increased by 39 ha as compared to 2014. Thus, 88 ha of dense forest was converted to sparse forest and 39 ha of sparse forest was converted to bare land as the result of drought. The result found that in 2016 the maximum dense forest was detected during the entire study period. Accordingly, 424 ha of dense forest was detected and increased by 207 ha. Sparse forest and bare land decreased this year. This indicated that sparse forests were rehabilitated and changed to the more dense forest while bare land was rehabilitated into the sparse forest during this time. Contrary to 2016, in 2017 dense forest was significantly decreased by 231 ha. Though the sparse forest was increased, the maximum bare land area was registered this year. As indicated by the above VCI result maximum extreme drought was registered in 2017. As the result, 100 ha of sparse forest was lost to drought this year as it's indicated in Table 4. In 2018 both dense forest and sparse forest increased and bare land decreased. This

Fig. 3 Spatial map of drought severity class

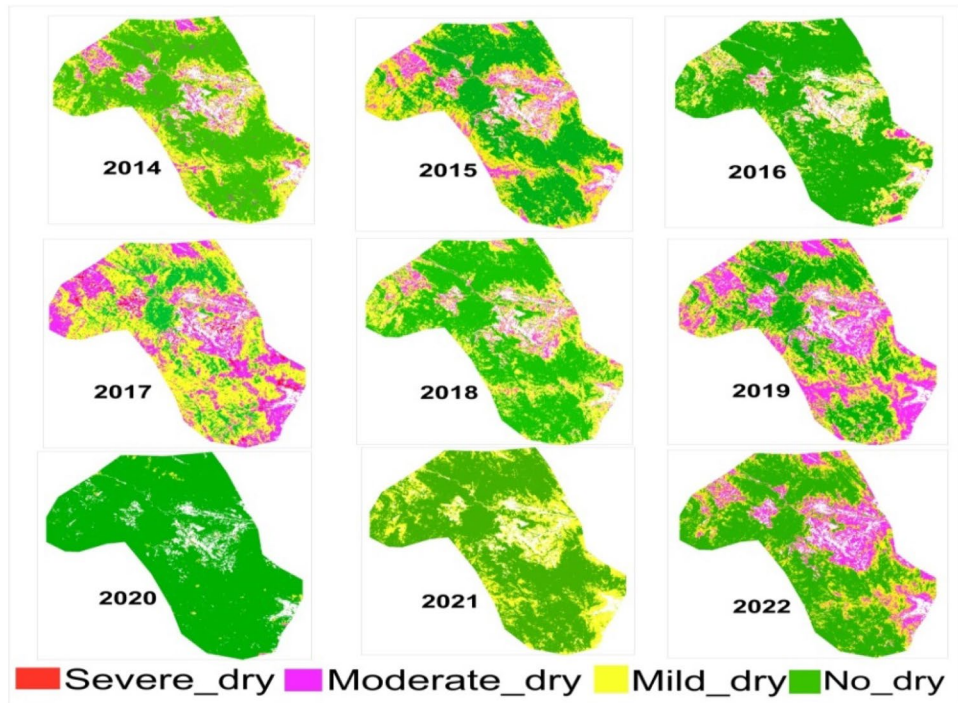


Table 3 Spatial extend of drought class during 2014–2022

Year	Severe(ha)	Moderate(ha)	Mild(ha)	Normal(ha)
2014	80.1	2048.8	7048.4	15,783.7
2015	177.5	2994.4	8691.9	13,097.2
2016	7.6	665.3	5240.3	19,048.7
2017	537.9	7116.2	12,887.5	4420.7
2018	43.6	1591.2	7744.7	15,581.2
2019	69.7	7359.7	8969.3	8563.7
2020	0	37.9	269.9	24,644.2
2021	0	4.3	6568.5	18,403.5
2022	80.6	4449.6	6050.3	14,381.4

Table 4 Forest covers change

Years	Dense forest(ha)	Sparse forest(ha)	Bare land(ha)
2014	305	19,660	4995
2015	217	19,709	5034
2016	424	19,575	4961
2017	193	19,718	5059
2018	372	19,986	4602
2019	232	19,823	4905
2020	374	19,685	4901
2021	380	19,904	4556
2022	327	19,821	4612

indicated that because the study area experienced normal climatic variables; vegetation was recovered during this time. Hence, the dense forest was increased by 179 ha, the sparse forest was increased by 268 ha and the bare land was decreased by 457 ha. This study found that drought that occurred at every interval of 2 years (2015, 2017, and 2019) brought significant change to forest resources. For instance, in 2019 dense forest and sparse forest decreased by 140 ha and 163 ha respectively as compared to 2018, and bare land increased by 303 ha. Following 2019 the two consecutive years thus 2020 and 2021 were experienced the normal year. Hence, both dense forests and sparse forests increased while bare land decreased. Contrary, in 2022 both

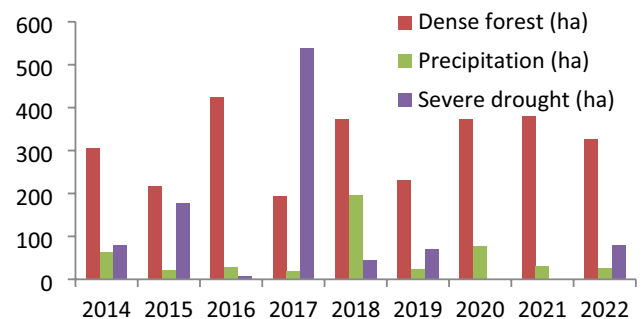
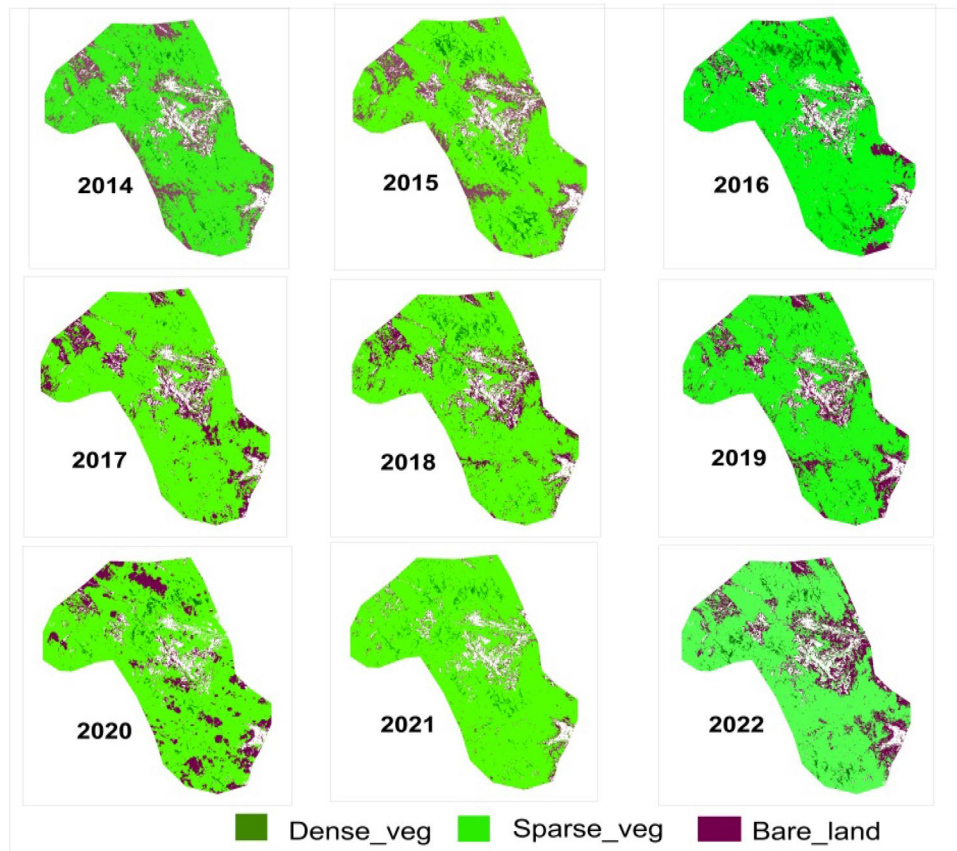


Fig. 4 Dense forest, Precipitation, and Severe drought trend during the study period

Fig. 5 Map of forest cover change



dense forest and sparse forest decreased whereas bare land increased.

The spatial mapping of the impacts of the major registered drought event in the study area during the study period showed that vegetation activity across the entire study area decreased, as drought occurred over the region (Fig. 4). Thus, the forest has not stables during the study period as the result of climate change. In all of the detected drought years, the dense and sparse forest was diminished through the Northwest, central, and southeast of the forest (Fig. 5).

To explicitly, illustrate the impact of drought on forest cover, the below histogram was used to indicate the trend of three variables that were purposively selected (Fig. 4).

3.3 Relationship between precipitation and forest

In this study, the relationship between precipitation and NDVI were examined to recognize how precipitation controls the function of environmental resource, particularly forest. The result of this finding showed that there is a positive correlation between precipitation and NDVI. The result of R^2 as shown in Fig. 6 is 0.49. Thus, 49% of NDVI that indicates vegetation condition can be determined by precipitation since the value of R^2 was 0.49 in this study

(Fig. 6). The regression analysis result also showed that the relationship between precipitation and NDVI is positive, ($R/P = 0.69/0.05$) and statistically significant. Thus, the results indicated that when the precipitation increases, NDVI also tends to increase. When precipitation deficit occurred in this Yabello forest region vegetation cover and greenness became decreased and vice versa. For instance, in 2018 mean precipitation of the short rainy season was 195 mm and highest as compared to other years during the study period. Also, vegetation greenness was high and the maximum NDVI value (0.27) was registered this year (Fig. 6).

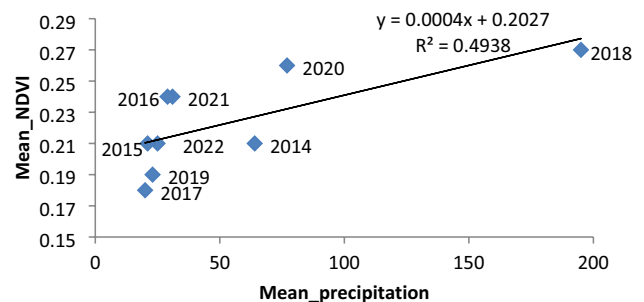


Fig. 6 Relationships between NDVI and Precipitation

4 Discussion

Northern, eastern, and southern regions of Ethiopia have been frequently affected by drought. The frequency of occurrence of drought is becoming beyond the loss of livestock and crop failure and resulting in forest degradation. As indicated in the VCI result, drought has occurred in the Yabello forest area nearly every two years. This finding is in line with several studies that projected drought occurrence in the lowland region of Ethiopia to have occurred every two to five years [38, 39]. Also, the Study conducted in the “Yabello and El-Woye area reported that Yabello districts had an extremely severe drought with SPI value—2.28 at a two-month timescale which belongs to the season of this study (September to October) in the 2015 drought year from 1987 to 2017 [40]. Similarly, the drought that occurred in 2017 resulted in severe damage to assets and exposed hundreds of thousands to famine and costs for relief as highlighted by [41]. According to the report of [42], the eastern Horn of Africa region has experienced drought conditions following consecutive poor seasons since late 2020 leading to significant impacts on production, vegetation, water resources, food insecurity, and livelihoods. In line with this report, the VCI result of this study indicated that vegetation greenness was beginning to decrease as precipitation deficit was reported for three consecutive seasons. Hence, drought severity appeared in the Yabello forest. This report stated the drought years of 2017 and 2019 in the southern region of Ethiopia which confirmed the result of this study.

Because of climate extremes like drought, the forest can be converted to bare land or the more dense forest can be sparsely distributed. Several studies reported as forest cover declined as a result of drought. For instance, a study conducted on forest cover change and climate variability in southern Ethiopia determined that the forest cover was decreasing from 10,020.3 ha to 8,851.2 ha, between 1986 and 2018 respectively as a result of climate change [43]. A similar study also found that forest cover was changed as a result of rising temperatures from 1990 to 2021 in Turkey [44]. The negative impact of rising of temperature along with drought is not only confined to the forest. but, it can cause migration/diminishing of species [5, 6] Likewise, in 2015, 2017, 2019, and 2022 drought brought the loss of many life stock productions in the Borana lowland region of Ethiopia. The drought resulted in the loss of 231 ha of dense forest and the loss of 100 ha of sparse forest in 2017 as compared to 2016 in the Yabello forest. The drought resulted in plant mortality as suggested by [30, 45]. But, based on vegetation types and structure the ways forests respond to drought are different. For instance, in this study dense forest was converted to sparse forest, and

sparse forest was lost to drought. This study also found that drought seriously diminished dense forests in the 2017 year (Table 4 and Fig. 5). In line with this finding, a study conducted on Taltele range land which is a neighbor of this study found that the larger change in land observed in forest, grassland, and wetland was detected during the period from 1995–2000 and 2015–2019, this is due to climate change impact happened in Taltele rangeland [21]. A similar study found that forest cover has shown variability from 1986 to 2018 in the Kafa zone using NDVI indices [43]. Also, [46] observed that vegetation activities decreased as drought appeared over Southeastern Europe using SPEI.

To conserve natural resources, knowing the relationship between drought indices plays a great role [47]. In the semi-arid region, precipitation is the most important one of the climate elements to recognize the biophysical environmental function. As a result, several studies examine the relationship between precipitation and NDVI to recognize how vegetation is stressed as a result of precipitation deficit [4, 11, 48]. Commonly, they found that positive relationship between precipitation and NDVI. Similarly, this study confirmed that precipitation variability is extra-ordinarily responsible for vegetation change in the Yabello forest, due to the dominant role that precipitation plays in water availability which has been considered as the principal factor controlling ecosystem structure and driving biological processes in vegetation. Thus, when precipitation is a deficit for the plant, the plant closes its stomata to conserve water. Hence, photosynthesis is no longer functions and plant mortality can be occurring (Fig. 6).

5 Conclusion

Climate extreme like drought is challenging the globe in multi-direction. Its negative impact adversely affects ecosystem function. Particularly its impact on forest resources is attracting the attention of many scholars, and decision-makers also required information regarding drought characteristics. This study proposed spatial and temporal analysis of drought evolution in the Yabello forest area in the lowland region of Ethiopia from 2014 to 2022. The results showed the usefulness of incorporating forest cover change in assessing the Spatio-temporal variability of drought severity in the dry-lands. Remote Sensing-based vegetation time series indices were used, as complementary to in-situ data indices. NDVI-based forest cover change and VCI Indicators were used for monitoring changes in vegetation conditions and drought severity during the growing seasons (September to November) from 2014–2022.

Results showed high temporal and spatial variability in vegetation cover between drought and non-drought

conditions in this study. The associated negative impact of droughts on the vegetation resulting in limited forest cover was further confirmed by results from this study. Severe drought occurred in 2015, 2017, 2019, and 2022 and forest cover was highly affected during these years. The wettest years were 2014, 2016, 2018, 2020, and 2021.

Simple linear regression analysis that considered precipitation as the independent variable and forest greenness as the dependent variable confirmed that half of the forest degraded was because of precipitation deficit. Due to a lack of precipitation, forest has been degraded every two years in this Yabello forest. This study highlighted drought impact as the most climate phenomenon that causes forest degradation in the semi-arid region of Ethiopia which requires policy actions toward climate change adaptation options. Moreover, future research should be integrating remote sensing metrics with other factors like socio-economic and biophysical data to assess drought magnitude and intensity in the study area.

Acknowledgements The authors acknowledged the United State Geological Survey (USGS) Organization for their freely offering satellite data.

Author contributions BNW: Investigation, Validation, Data Curation, Writing—Original Draft, Writing—Review & Editing. FGG: Conceptualization, Methodology, Software, Data Curation & Editing.

Funding The authors declare that no funds, grants, or other support were received during the preparation of this manuscript.

Data availability All data are available from the corresponding author upon reasonable request.

Declarations

Conflict of interest The authors have no competing interests to declare that are relevant to the content of this article.

Open Access This article is licensed under a Creative Commons Attribution 4.0 International License, which permits use, sharing, adaptation, distribution and reproduction in any medium or format, as long as you give appropriate credit to the original author(s) and the source, provide a link to the Creative Commons licence, and indicate if changes were made. The images or other third party material in this article are included in the article's Creative Commons licence, unless indicated otherwise in a credit line to the material. If material is not included in the article's Creative Commons licence and your intended use is not permitted by statutory regulation or exceeds the permitted use, you will need to obtain permission directly from the copyright holder. To view a copy of this licence, visit <http://creativecommons.org/licenses/by/4.0/>.

References

- Madani N, Kimball JS, Jones LA, Parazoo NC, Guan K (2017) Global analysis of bioclimatic controls on ecosystem productivity using satellite observations of solar-induced chlorophyll fluorescence. *Remote Sens* 9(6):530. <https://doi.org/10.3390/rs90605302>
- Xu HJ, Wang XP, Zhao CY, Yang XM (2020) Assessing the response of vegetation photosynthesis to meteorological drought across northern China. *Land Degrad Dev* 32(1):20–34. <https://doi.org/10.1002/ldr.3701>
- Manzoni S, Katul G, Porporato A (2014) A dynamical system perspective on plant hydraulic failure. *Water Resour Res* 50(6):5170–5183. <https://doi.org/10.1002/2013WR015236>
- Vicente-Serrano SM, Gouveia C, Camarero JJ, Beguería S, Trigo R, López-Moreno JJ, Sanchez-Lorenzo A (2013) Response of vegetation to drought time-scales across global land biomes. *Proc Natl Acad Sci* 110(1):52–57. <https://doi.org/10.1073/pnas.1207068110>
- Tekin O, Cetin M, Varol T, Ozel HB, Sevik H, Zeren Cetin I (2022) Altitudinal migration of species of Fir (*Abies* spp.) in adaptation to climate change. *Water, Air, Soil Pollut* 233(9):385. <https://doi.org/10.1007/s11270-022-05851-y>
- Varol T, Canturk U, Cetin M, Ozel HB, Sevik H, Zeren Cetin I (2022) Identifying the suitable habitats for Anatolian boxwood (*Buxus sempervirens* L.) for the future regarding the climate change. *Theor Appl Climatol* 150(1–2):637–647. <https://doi.org/10.1007/s00704-022-04179-1>
- Barros C, Thuiller W, Münkemüller T (2018) Drought effects on the stability of forest-grassland ecotones under gradual climate change. *PLoS ONE* 13(10):e0206138. <https://doi.org/10.1371/journal.pone.0206138>
- Pandey PC, Arellano P (eds) (2022). Wiley, New York
- Jingyong Z, Wenjie D, Congbin F, Lingyun W (2003) The influence of vegetation cover on summer precipitation in China: a statistical analysis of NDVI and climate data. *Adv Atmos Sci* 20(6):1002–1006. <https://doi.org/10.1007/BF02915523>
- Rembold F, Maselli F (2006) Estimation of inter-annual crop area variation by the application of spectral angle mapping to low resolution multitemporal NDVI images. *Photogramm Eng Remote Sens* 72(1):55–62. <https://doi.org/10.14358/PERS.72.1.55>
- Akinyemi FO (2021) Vegetation trends, drought severity and land use-land cover change during the growing season in semi-arid contexts. *Remote Sens* 13:836. <https://doi.org/10.3390/rs13050836>
- Chen Z, Wang W, Fu J (2020) Vegetation response to precipitation anomalies under different climatic and biogeographical conditions in China. *Sci Rep* 10(1):1–16. <https://doi.org/10.1038/s41598-020-57910-1>
- Nemani RR, Keeling CD, Hashimoto H, Jolly WM, Piper SC, Tucker CJ, Running SW (2003) Climate-driven increases in global terrestrial net primary production from 1982 to 1999. *Science* 300(5625):1560–1563. <https://doi.org/10.1126/science.1082750>
- Notaro M, Liu Z, Gallimore RG, Williams JW, Gutzler DS, Collins S (2010) Complex seasonal cycle of ecohydrology in the Southwest United States. *J Geophys Res: Biogeosci*. <https://doi.org/10.1029/2010Jg001382>
- Gidey E, Dikinya O, Sebego R, Segosebe E, Zenebe A (2018) Analysis of the long-term agricultural drought onset, cessation, duration, frequency, severity and spatial extent using Vegetation Health Index (VHI) in Raya and its environs. *North Ethiopia Environ Syst Res* 7(1):1–18. <https://doi.org/10.1186/s40068-018-0115-z>
- Kourouma JM, Eze E, Negash E, Phiri D, Vinya R, Girma A, Zenebe A (2021) Assessing the spatio-temporal variability of NDVI and VCI as indices of crops productivity in Ethiopia: a remote sensing approach *Geomatics*. *Nat Hazards Risk*. <https://doi.org/10.1080/19475705.2021.1976849>

17. Muir C, Southworth J, Khatami R, Herrero H, Akyapı B (2021) Vegetation dynamics and climatological drivers in Ethiopia at the turn of the century. *Remote Sens* 13(16):3267. <https://doi.org/10.3390/rs13163267>
18. Liou YA, Muluaem GM (2019) Spatio-temporal assessment of drought in Ethiopia and the impact of recent intense droughts. *Remote Sens* 11(15):1828. <https://doi.org/10.3390/rs11151828>
19. Wolteji BN, Bedhadha ST, Gebre SL, Alemayehu E, Gemedo DO (2022) Multiple indices based agricultural drought assessment in the Rift Valley region of Ethiopia. *Environ Chall* 7:100488. <https://doi.org/10.1016/j.envc.2022.100488>
20. Hundera H, Berhan G, Bewuket W (2016) Remote sensing and GIS based agricultural drought risk assessment in East Shewa Zone, Central Rift Valley Region of Ethiopia. *Remote Sens* 6(7):48–54
21. Fenetahun Y, Yong-Dong W, You Y, Xinwen X (2020) Dynamics of forage and land cover changes in Teltele district of Borana rangelands, southern Ethiopia: using geospatial and field survey data. *BMC Ecol* 20(1):1–16. <https://doi.org/10.1186/s12898-020-00320-8>
22. Gifawesen ST, Feyssa DH, Feyissa GL (2020) Analysis of forest cover change in Yabello Forest, Borana Zone, Ethiopia. *Int J Biodivers Conserv* 12(4):350–362. <https://doi.org/10.5897/ijbc2018.1222>
23. Negassa MD, Mallie DT, Gemedo DO (2020) Forest cover change detection using Geographic Information Systems and remote sensing techniques: a spatio-temporal study on Komto Protected forest priority area, East Wollega Zone. *Ethiopia Environ Syst Res* 9(1):1–14. <https://doi.org/10.1186/s40068-020-0163-z>
24. Awoke BG (2010) The role of geo information technology for predicting and mapping of forest cover spatio-temporal variability: Dendi district case study, Ethiopia. *J Sustain Dev Afr* 12(6):9–33
25. NASA Shuttle Radar Topography Mission (SRTM) (2013) Shuttle Radar Topography Mission (SRTM) Global. *Distrib OpenTopography*. <https://doi.org/10.5069/G9445JDF>
26. Worku MA, Feyisa GL, Beketie KT (2022) Climate trend analysis for a semi-arid Borana zone in southern Ethiopia during 1981–2018. *Environ Syst Res* 11(1):1–20. <https://doi.org/10.1186/s40068-022-00247-7>
27. Coppock DL (Ed.) (1994) The Borana plateau of southern Ethiopia: synthesis of pastoral research, development, and change, 1980–1991 (Vol 5). ILRI (aka ILCA and ILRAD). <https://hdl.handle.net/10568/4660>
28. Jaleta D, Lemenih M, & Lemma B (2010) Extent of bush encroachment and its impacts on selected soil properties in Borana rangeland, Ethiopia (Doctoral dissertation, Wondo Genet College of Forestry and Natural Resources, Hawassa University)
29. Central Statistical Agency (CSA) (2013) Federal democratic republic of Ethiopia. Population projection of Ethiopia for all regions at Woreda level from 2014–2017. Addis Ababa
30. Ji L, Peters AJ (2003) Assessing vegetation response to drought in the northern Great Plains using vegetation and drought indices. *Remote Sens Environ* 87(1):85–98. [https://doi.org/10.1016/S0034-4257\(03\)00174-3](https://doi.org/10.1016/S0034-4257(03)00174-3)
31. Funk C, Peterson P, Landsfeld M, Pedreros D, Verdin J, Shukla S, Michaelsen J (2015) The climate hazards infrared precipitation with stations—a new environmental record for monitoring extremes. *Sci Data* 2(1):1–21. <https://doi.org/10.1038/sdata.2015.66>
32. Bayissa YA, Tadesse T, Svoboda M, Wardlow B, Poulsen C, Swigart J, Van Andel SJ (2019) Developing a satellite-based combined drought indicator to monitor agricultural drought: a case study for Ethiopia. *GISci Remote Sens* 56(5):718–748. <https://doi.org/10.3390/rs9070669>
33. Ayehu GT, Tadesse T, Gessesse B, Dinku T (2018) Validation of new satellite rainfall products over the Upper Blue Nile Basin Ethiopia. *Atmos Meas Tech* 11(4):1921–1936. <https://doi.org/10.5194/amt-11-1921-2018>
34. Bayissa Y, Tadesse T, Demisse G, Shiferaw A (2017) Evaluation of satellite-based rainfall estimates and application to monitor meteorological drought for the Upper Blue Nile Basin. *Ethiopia Remote Sens* 9(7):669. <https://doi.org/10.3390/rs9070669>
35. Tucker CJ (1979) Red and photographic infrared linear combinations for monitoring vegetation. *Remote Sens Environ* 8(2):127–150. [https://doi.org/10.1016/0034-4257\(79\)90013-0](https://doi.org/10.1016/0034-4257(79)90013-0)
36. Kogan FN (1995) Application of vegetation index and brightness temperature for drought detection. *Adv Space Res* 15(11):91–100. [https://doi.org/10.1016/0273-1177\(95\)00079-T](https://doi.org/10.1016/0273-1177(95)00079-T)
37. Athick AMA, Shankar K, Naqvi HR (2019) Data on time series analysis of land surface temperature variation in response to vegetation indices in twelve Wereda of Ethiopia using mono window, split window algorithm and spectral radiance model. *Data Brief* 27:104773. <https://doi.org/10.1016/j.dib.2019.104773>
38. Mera GA (2018) Drought and its impacts in Ethiopia. *Weather Clim Extrem* 22:24–35. <https://doi.org/10.1016/j.wace.2018.10.002>
39. Gizachew L, Shimelis A (2014) Analysis and mapping of climate change risk and vulnerability in Central Rift Valley of Ethiopia. *Afr Crop Sci J* 22:807–818. <https://doi.org/10.13140/RG.2.1.1671.1209>
40. Duba GW, Demissie ST, Emiru TS (2021) Meteorological droughts from 1987–2017 in Yabello and El-Woye areas of Borana, Oromia Region, Ethiopia. *Ethiop J Soc Sci* 7(1):72–86
41. Tafesse B (2021) Role of pastoralists' indigenous knowledge in drought risk reduction: implications for early warning system and adaptation practices in Borana, Southern Ethiopia. *Ethiop J Agric Sci* 31(3):41–52
42. FAO/WFP (2022) Regional Bureau for Eastern Africa Research, Analysis & Monitoring (Ram) Unit; Status of Drought Across the Eastern Horn of Africa. <https://docs.wfp.org/api/documents/WFP-0000141001/download/>
43. Lemma DB, Gebretsadik KT, Debela SK (2021) Forest cover change detection in relation to climate variability and LULC changes using GIS and RS techniques. A case of the Kafa zone, southwest Ethiopia. *J Water Land Dev*. <https://doi.org/10.24425/jwld.2021.139025>
44. Shimizu K, Ota T, Mizoue N (2019) Detecting forest changes using dense Landsat 8 and Sentinel-1 time series data in tropical seasonal forests. *Remote Sens* 11(16):1899. <https://doi.org/10.3390/rs11161899>
45. Tadesse T, Bayissa YA, Scoboda M, Fuchs B, Zhang B, Demisse G, Wardlow B, Bohrer G, Clark K, Desai A, Gu L, Noormets A, Novick K, Richardson A (2020) Forest Drought Response Index (ForDRI): a new combined model to monitor forest drought in the Eastern United States. *Papers Nat Res*. <https://doi.org/10.3390/rs12213605>
46. Páscoa P, Gouveia CM, Russo AC, Bojariu R, Vicente-Serrano SM, Trigo RM (2020) Drought Impacts on Vegetation in Southeastern Europe. *Remote Sens* 12(13):2156. <https://doi.org/10.3390/rs12132156>
47. Gidey E, Dikinya O, Sebego R, Segosebe E, Zenebe A (2018) Using drought indices to model the statistical relationships between meteorological and agricultural drought in Raya and its environs. *North Ethiopia Earth Syst Environ* 2(2):265–279. <https://doi.org/10.1007/s41748-018-0055-9>
48. Zhang L, Xiao J, Zhou Y, Zheng Y, Li J, Xiao H (2016) Drought events and their effects on vegetation productivity in China. *Ecosphere* 7(12):e01591. <https://doi.org/10.1002/ecs2.1591>

Publisher's Note Springer Nature remains neutral with regard to jurisdictional claims in published maps and institutional affiliations.